X-RAY FINGERPRINTING ROUTINE FOR CUT DIAMONDS

Roland Diehl and Nikolaus Herres

X-ray topography is a nondestructive technique that permits the visualization of internal defects in the crystal lattice of a gemstone, especially diamond, which is highly transparent to X-rays. This technique yields a unique "fingerprint" that is not altered by gem cutting or treatments such as irradiation and annealing. Although previously a complicated and time-consuming procedure, this article presents a simplified X-ray topographic routine to fingerprint faceted diamonds. Using the table facet as a point of reference, the sample is crystallographically oriented in a unique and reproducible way in front of the X-ray source so that only one topograph is necessary for fingerprinting. Should the diamond be retrieved after loss or theft, even after recutting or exposure to some forms of treatment, another topograph generated with the same routine could be used to confirm its identity unequivocally.

Diamonds, whether rough or cut (figure 1), are one of the most closely scrutinized commodities in the world. Gemological laboratories routinely evaluate the carat weight, color, clarity, and cut characteristics of faceted diamonds, and record them on a report that serves not only as a basis for the gem's value, but also as a record that can help in the later identification of a stone. These identifying characteristics may be useful in the event of loss or theft, and for tracking diamonds that may be resubmitted to laboratories for regrading. However, re-identification may become difficult or impossible if the stone has undergone any of the following:

- Re-cutting or re-polishing, which may cause significant deviations in a stone's proportions and weight, or remove identifying marks such as laser inscriptions
- Laser drilling, which can significantly change the clarity appearance and/or grade
- Treatments to induce a change in color

In the past decade, there have been various attempts to develop characterization methods that render a faceted diamond uniquely identifiable. One method records the pattern of light reflected from the facets on a cylindrical sheet of film surrounding the stone. Such a *scintillogram* is indeed a "fingerprint," but minor re-polishing will modify subsequent patterns obtained from the same stone (Wallner and Vanier, 1992). Another approach is to place a mark on the surface of a given stone that does not affect its clarity grade, but is clearly visible under certain viewing conditions. As described in a recent patent (Smith, 1999), this type of feature can be generated by ion-beam milling to "uniquely identify the gemstone by a serial number or as a brand or quality mark." However, the mark penetrates only about 30 nm, so it can be easily polished away with just a tiny loss in weight. In at least one instance, laser inscriptions were polished off diamonds that had been decolorized by high pressure/high temperature treatment (Moses et al.,

See end of article for About the Authors and Acknowledgments.
GEMS & GEMOLOGY, Vol. 40, No. 1, pp. 40–57.

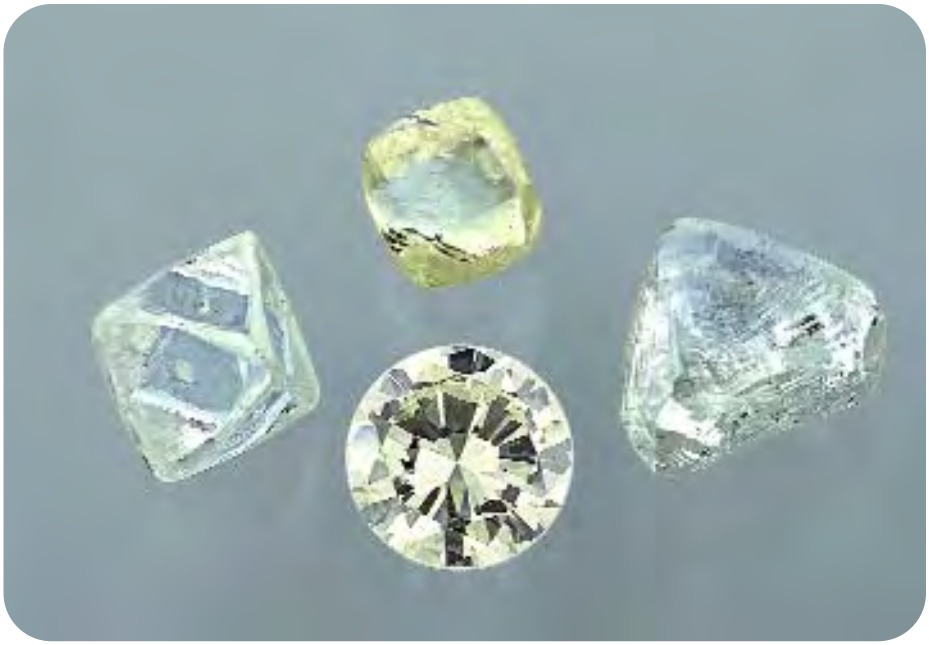

Figure 1. Diamond crystals show morphological features, such as sharp or resorbed crystal faces, that can be used to find the orientation of their crystal lattice. When faceted, the orientation of the crystal lattice relative to any facet can be described using X-ray topography. This technique also can be used to image various lattice defects, which form a unique "fingerprint" for each diamond. Clockwise from the 7.51 ct round brilliant is a 15.98 ct octahedron, a 9.43 ct yellow crystal, and a 22.32 ct macle (GIA Collection nos. 8992, 11954, 11952, and 11955, respectively). Photo by C. D. Mengason.

1999). In the last few years, advanced methods of fingerprinting diamonds have been researched to support a global certification program to deal with conflict diamonds (see, e.g., Laurs, 2001).

Most promising are X-ray methods, which can nondestructively portray the internal defects of a diamond's crystal lattice (figure 2), and have already been used to prove that two diamonds were faceted from the same piece of rough (Sunagawa et al., 1998). In this article, we present the concept of an alignment procedure using X-ray topography that routinely enables the unique and virtually unchangeable characterization of cut diamonds. We first described this concept, in German, in the late 1990s (Diehl and Herres, 1997; 1998); it was based on the study of one piece of rough and three faceted diamonds (one of which was cut from the sample piece of rough), from which we collected approximately 50 topographs.

To explain the essentials of this concept here, we have provided some background on crystallography. The first section below describes how the individual faces of crystal forms are named. The next introduces the most important crystal forms of diamond and their symmetry, and the third explains the representation of a crystal's orientation using a stereographic projection. Then, following an introduction to crystal lattice defects and some basics of X-ray diffraction, we explain how to visualize lattice defects using X-ray topography. Finally, we describe the simplified routine to orient a faceted diamond for fingerprinting.

BACKGROUND

Directions and Faces in a Crystal Lattice. In principle, a crystal is a periodic regular arrangement of atoms in three dimensions. This spatial arrangement of atoms is termed a *crystal lattice*. In diamond, these atoms are carbon. During crystal growth, atoms are deposited layer by layer on lattice planes, causing the crystal to grow as the lattice planes increase in area. When the crystal stops growing, the multitude of lattice planes forms the faces, edges, and corners of the crystal (figure 3).

In crystallography, a system of axial coordinates is used to index the individual faces of a crystal so that it can be described completely. To achieve this, crystallographers denote the faces of a crystal form with numerals in parentheses called *Miller indices*. Crystal forms belonging to the cubic system—such as the cube, octahedron, and dodecahedron—are related to a perpendicular set of coordinate axes x, y, and z, with faces that intersect these axes at equal units a, b, and c (figure 4). The Miller indices (hkl) describe the position of a crystal face relative to the distance at which it intersects each of the coordinate axes. The index "h" refers to the x-axis, "k" to the y-axis, and "l" to the z-axis.

Consider face A in figure 4, which intersects the x-axis at 1a and the y-axis at 1b, and is parallel to the z-axis (which means that it intersects the z-axis at infinity, ∞). As calculations with infinite numbers are inconvenient, the axial intersections "1 1 ∞" are transformed to their reciprocal values to become "(110)" (read "one, one, zero"), which are the Miller

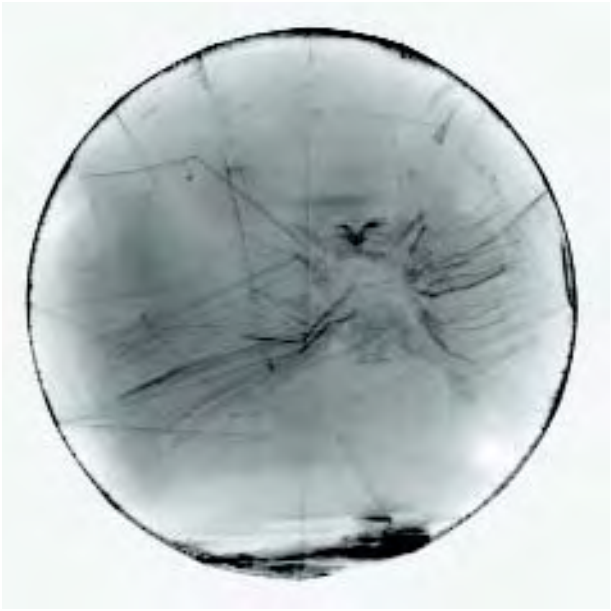

Figure 2. This X-ray topograph of a 0.63 ct round brilliant diamond shows characteristic bundles of dislocation lines and other contrast features that originate from lattice defects. Some of the pavilion edges also are visible as straight lines.

indices of crystal face A. Face B has the Miller indices (001), since it intersects the z-axis but not the x- or y-axes. Face C intersects all axes at the same relative distance, denoted (111). Face D, with its axial intersections of 1a, 2b, and $1^1/_2$c, transforms to "1, $^1/_2$, and $^2/_3$." However, Miller indices are always expressed as whole numbers, so multiplying by the common denominator (in this case 6) yields Miller indices for face D of (634).

Face E intersects the "positive" x-axis, the "negative" y-axis, and the "positive" z-axis, all at unity. Hence, the Miller indices of E are $(1\bar{1}1)$, read "one, bar one, one." Face F intersects the axes at 1a, 2b, and –2c, with reciprocal values of 1, $^1/_2$ and $-^1/_2$, respectively. After multiplication with a factor of 2 (again, the common denominator) to obtain integers, this yields the Miller indices $(21\bar{1})$.

The *orientation of vectors* within a crystal lattice is expressed within square brackets. The vector direction is defined according to the coordinate axes, starting at their intersection point or origin. For example, [100] denotes the direction parallel to the x-axis, and [111] denotes a diagonal direction (go 1a along x, 1b along y, and 1c along z, and connect this point with the origin of the coordinate axes). In a cubic lattice, a vector given by [hkl] is perpendicular to the (hkl) plane. [For textbooks on crystallography, see, for example, Buerger (1967) and Borchardt-Ott (1997).]

Crystal Forms and Symmetry. An inherent property of regular crystal forms is their symmetry (figure 5). This is recognized by their congruence of shape when viewed from various directions. Thus, when viewed parallel to one of its three coordinate axes, a cube looks like a square (figure 6); the appearance of a square occurs six times (twice for each coordinate axis). This multiplicity is eight-fold for an octahedron and 12-fold for a dodecahedron. The crystal faces of these highly symmetric forms are described as "symmetrically equivalent," and a single index can be used to express the form of the crystal as a whole. When this is done, the index is placed in braces, for example {100} for a cube.

The cube, also known as a "hexahedron," has six faces with Miller indices (100), (010), (001), $(\bar{1}00)$, $(0\bar{1}0)$, and $(00\bar{1})$—indicating that each face intersects only one of the coordinate axes, but is parallel to the remaining two axes. This ensemble of faces is symbolized by {100} for this crystal form. The octahedron—the crystal form of most diamonds—is represented by {111}, since the axes are intersected at equal length by each of the eight faces.

Each of the 12 faces of the dodecahedron intersects two of the axes at equal length and does not

Figure 3. This schematic illustration shows a diamond octahedron in relation to the underlying crystal lattice. Such octahedra usually have a rounded appearance due to partial dissolution after crystal growth.

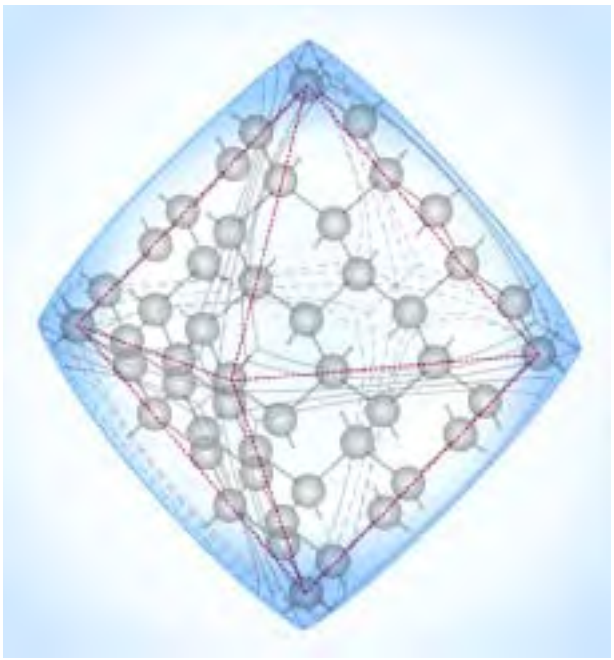

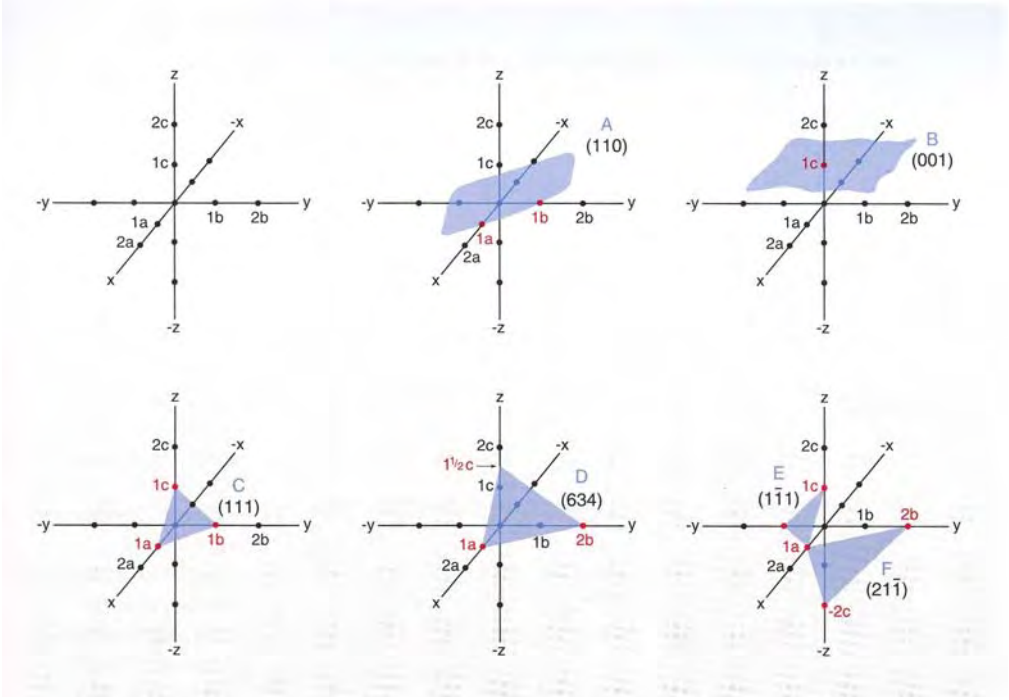

Figure 4. Crystal forms belonging to the cubic system (such as diamond) are related to a perpendicular set of coordinate axes x, y, and z. Crystal faces are described by Miller indices according to their intersection with these axes at unit distances of a, b, and c, respectively. (See text for details.)

intersect the third axis. Hence the Miller index for this crystal form is {110}. The dodecahedron is another important crystal form of diamond; it is thought to form by post-growth resorption along the edges of an octahedron.

Another way to express symmetry is to relate a crystal form to rotation around imaginary axes that run through the intersection point (or "origin") of the coordinate axes. For a cube, there are three such perpendicular axes, each connecting the center of one square face to the center of the opposite face. With each complete rotation of the cube around one axis, there are four positions of congruence—that is, after each quarter-turn, the cube looks like it did in the previous position. This axis of four-fold symmetry is called a *tetrad*. A cube has three tetrads, which coincide with the three coordinate axes.

An axis that connects two corners of a cube exhibits three positions of congruence after a full rotation of the cube. This three-fold symmetry axis is termed a *triad*. Since a cube has eight corners, it has four triads.

An axis that connects the centers of opposite cube edges has two-fold symmetry. These are termed *diads* because congruence occurs after each half-turn. A total of six diads connect the 12 edges of a cube.

Octahedra and dodecahedra exhibit the same axial symmetry as a cube. Tetrads connect the corners of the octahedron, triads connect the centers of its opposing faces, and diads connect the centers of its edges. For the dodecahedron, tetrads connect the acute corners, triads connect the obtuse corners, and diads connect the centers of its faces.

Complementing axial symmetry, mirror symme-

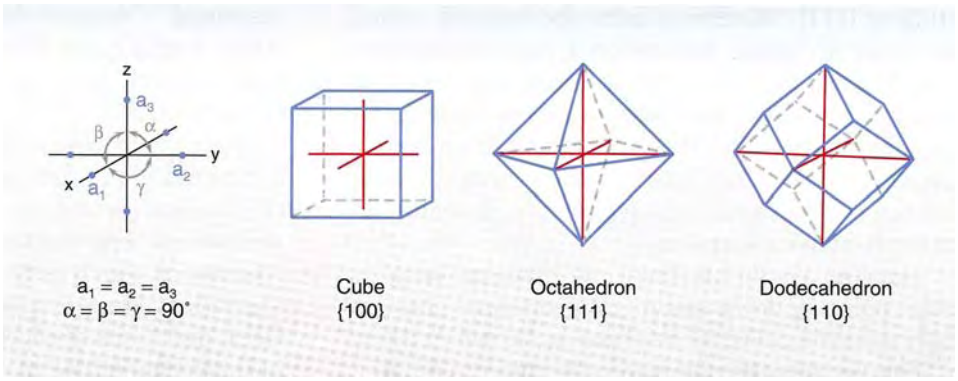

Figure 5. The cubic system has the highest degree of symmetry of all the crystal systems. All three axes are perpendicular, and the unit distances a, b, and c are equal and therefore commonly denoted a_1, a_2, and a_3 to indicate equality. Three common cubic forms are shown here. Diamond commonly displays octahedral and dodecahedral forms.

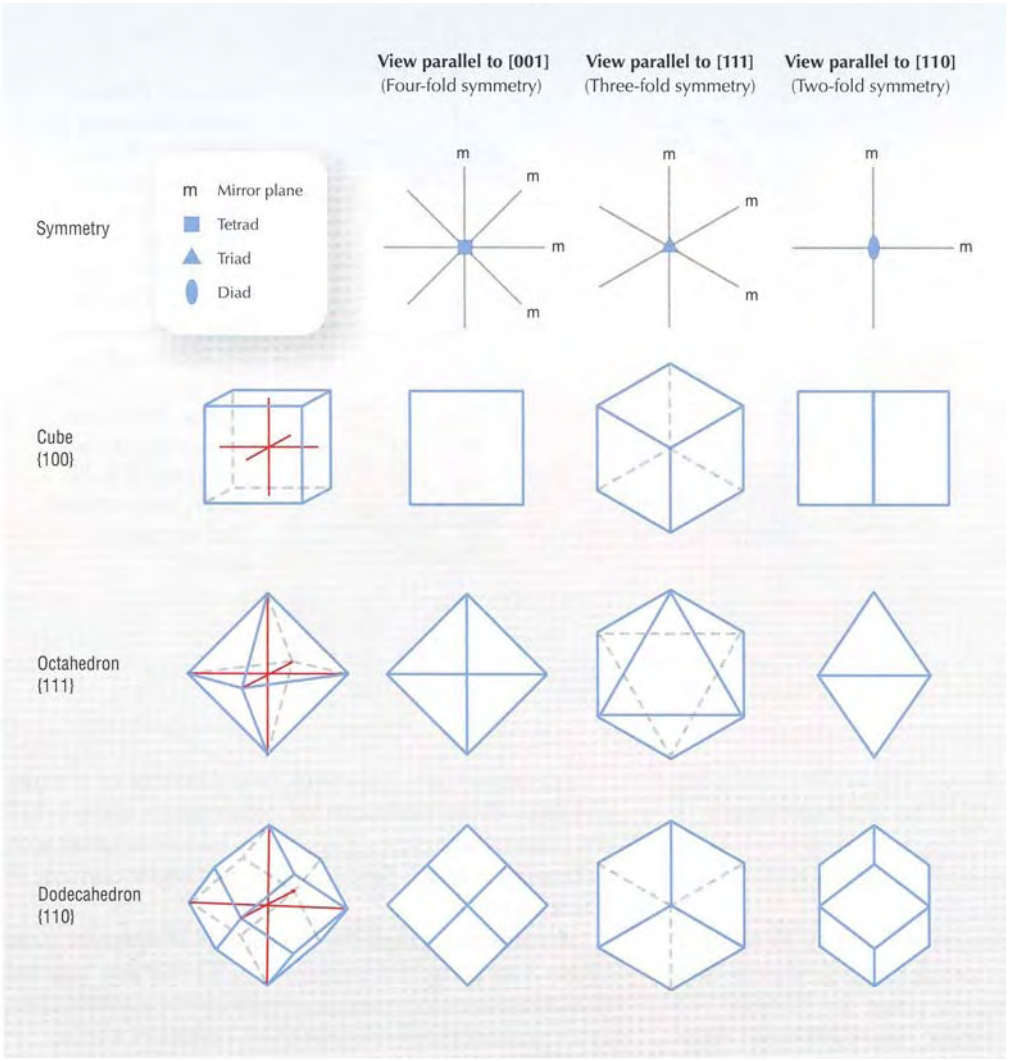

Figure 6. Depending on the viewing orientation, a variety of shapes and symmetries are apparent for these common cubic forms. The symmetry of these forms is shown according to mirror planes and rotational order (i.e., diad, triad, and tetrad for two-, three-, and four-fold rotational symmetry).

try relates two halves of a crystal form by a virtual plane termed a *mirror plane*. A total of nine mirror planes yield congruence of the cubic, octahedral, and dodecahedral crystal forms (again, see figure 6).

Mapping of Orientations Using Stereographic Projection. Most facets of a cut diamond are not parallel to low-index crystal lattice planes such as {100} or {111}. Moreover, since the original crystal faces are no longer present on a faceted diamond, the orientation of the crystal lattice in relation to the cut gemstone is obscured. X-ray techniques may be used to find this orientation, thus revealing the relationship between the polished facets, former crystal faces, lattice planes, and vectors in three-dimensional space.

Imagine a round brilliant cut diamond with its culet pointing down and its table oriented horizontally near the center of a sphere, as shown in figure 7. The vector perpendicular (or *normal*) to an arbitrarily chosen low-index crystal face present on the original crystal, such as {111}, will point from the center of the diamond to a point (or *pole*) on the sphere's surface. The location of this point can be described using two coordinates: ρ—the polar distance, expressed in degrees, relative to the "north pole" where the vertical diameter line intersects the sphere's surface; and φ—the azimuthal angle, measured in degrees along the horizontal diameter circle, starting at a point ("east pole") on the right side where a horizontal diameter line hits the sphere's surface.

Projecting a pole from the sphere's surface onto a horizontal plane that passes through the center of the sphere (as shown in figure 7) yields a two-dimensional representation of this crystal face, the position of which is given by polar distance ρ and azimuth φ. Projecting other crystal features such as faces, directions of edges, and/or vectors and planes in the crystal lattice in a similar fashion results in a

stereographic projection of these elements. The stereographic projection has many useful properties and applications beyond the scope of this article (for more on stereographic projections see, e.g., McKie and McKie, 1974, and Borchardt-Ott, 1997). We use such projections to graphically depict the orientation of a cut diamond (e.g., the diamond's table facet) relative to its crystal lattice.

In fact, it is possible to map the location of every facet of a cut diamond on a stereographic projection. Combined with knowledge of the relationship to crystal vectors within this projection (as acquired, e.g., by X-ray diffraction methods), projecting all of the facets of a particular cut diamond relative to its crystal lattice yields a unique depiction of that stone. However, even a slight repolishing of the stone would destroy the integrity of the data.

Figure 8 shows stereographic projections of {100}, {111}, and {110} faces; the axial symmetry at each crystal face pole is indicated by the shape of the symbols. The symmetry of a crystal is evident in these stereographic projections in much the same way as figure 6 shows this symmetry head-on. Owing to symmetry, a section of the cubic stereographic projection that covers only $^{1}/_{24}$ of the area of the projection plane is sufficient to describe a particular crystal form completely (the rest being possible to generate by symmetry operations), because both crystal form and crystal lattice have the same coordinate system.

This section is called a "standard triangle," denoted "t" in figure 8, which spans between poles generated by the normals to the neighboring faces (100), (111), and (110). The location of a pole (ρ,φ) within the frame of the standard triangle allows one to identify the orientation of a particular facet (e.g., the table facet) of a diamond with respect to the crystal lattice. Thus, to fix the orientation of the diamond's table facet with respect to the crystal lattice, the analyst must first determine the location of the pole of the perpendicular T to that facet within the standard triangle. This is accomplished by means of X-rays diffracted by the crystal lattice of the diamond. The diffraction of X-rays by single crystals—whether faceted or not—to yield spatial resolution of peculiarities within the crystal is called X-ray topography (see below for details). In contrast, X-ray powder diffraction is used to identify mineral species based on their specific powder diffraction patterns, which arise from the spacing and other characteristics of their lattice planes.

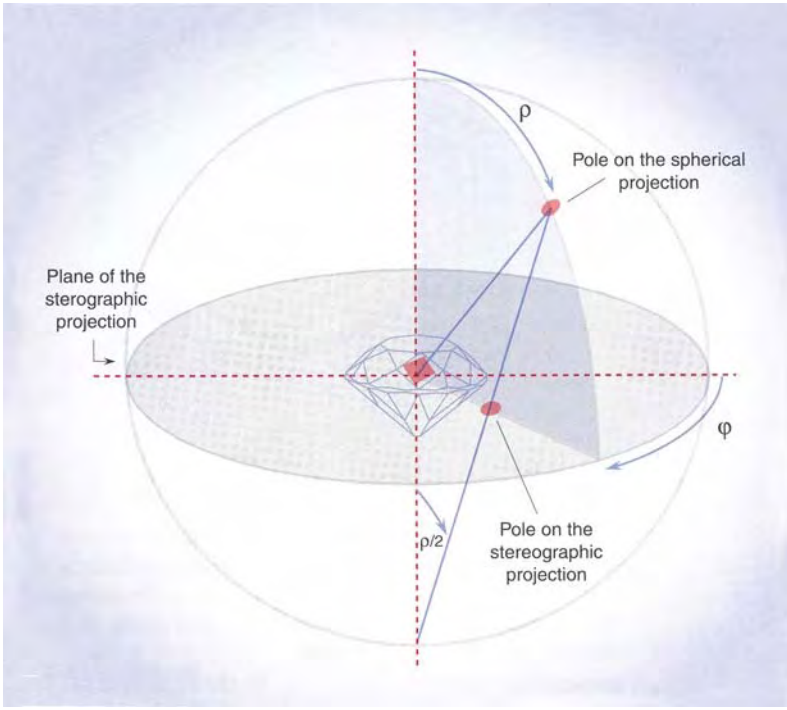

Figure 7. This diagram shows the mechanics of a stereographic projection. The orientation of the diamond crystal lattice is schematically shown within a round brilliant with its table oriented horizontally. A vector perpendicular to a certain crystal face, such as (111), will intersect the sphere's surface at a point called a pole. The location of the pole is described using two angular measurements, the polar distance ρ and the azimuthal angle φ. This pole is plotted on a stereographic projection by projecting its intersection with the sphere onto a horizontal plane that passes through the sphere's center.

Figure 8. These stereographic projections show the major cubic system faces projected along [001], [111], and [110] directions. Also shown is the "standard triangle" t (see text). The axial symmetry at each crystal face pole is indicated by the shape of the symbols: ■ = tetrad [100], ▲ = triad [111], and ▮ = diad [110].

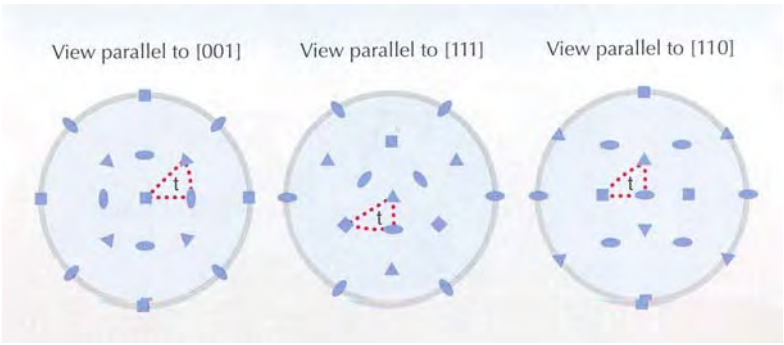

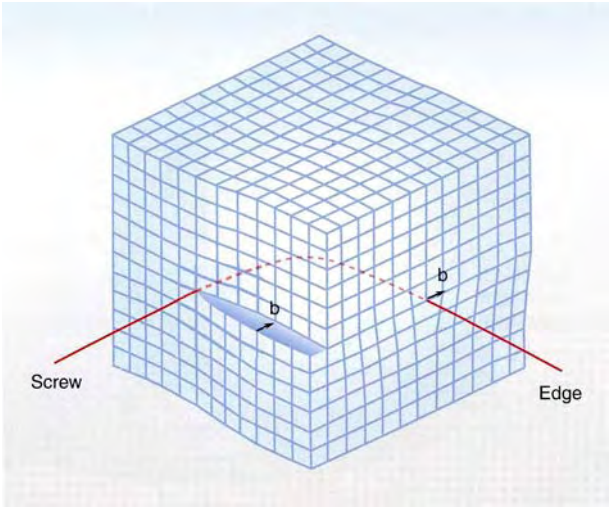

Figure 9. Crystal defects that extend over a relatively large portion of the crystal lattice are termed dislocations. *Most common are edge and screw dislocations. An edge dislocation occurs when a lattice plane is displaced by "one step," characterized by the displacement vector "b," as shown on the right side of the figure. For a screw dislocation, two lattice blocks are displaced against each other by "one step," again characterized by the displacement vector b, as shown on the left side. Both types of dislocations are accompanied by strain, which is revealed by diffracted X-rays, since the diffraction condition is not satisfied in the strained region of the lattice.*

Figure 10. A stacking fault, shown here in a diamond lattice, occurs when one portion of a crystal has a different orientation from the rest of that crystal. This change in the stacking sequence of the lattice planes is often the cause of twinning.

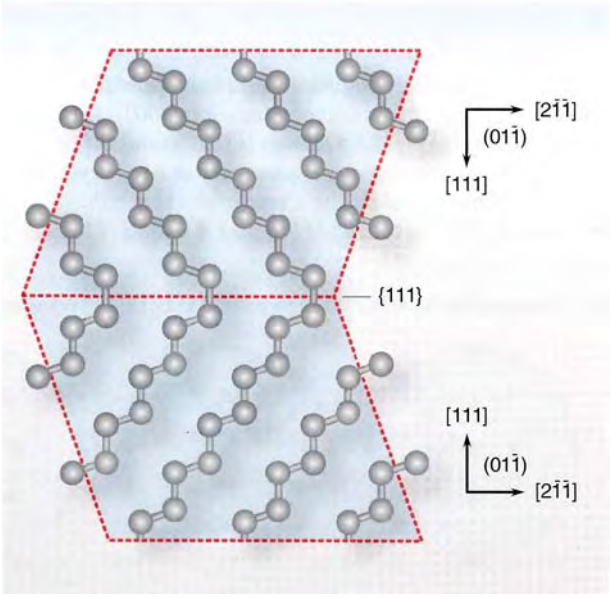

CRYSTAL LATTICE DEFECTS

As crystals grow layer by layer, this process almost never remains undisturbed. In reality, the regular spatial arrangement of atoms in a crystal lattice is locally perturbed by numerous defects of various kinds (Bohm, 1995; Kelly et al., 2000). Missing or additional atoms, atoms in wrong positions, or foreign atoms not belonging to the chemical composition of the crystal, are termed *point defects* or *centers*. Their presence is detected by physical or spectroscopic evidence. Due to lack of resolution, point defects cannot be detected by X-ray topography unless they cause regions of strain in the lattice around the defect. An even higher degree of disorder is caused by clusters of atoms of foreign phases or minerals, such as inclusions. Crystal lattice distortions that affect some local volume of the lattice are termed *extended defects* or *dislocations*. The most common types of extended defects are edge and screw dislocations (figure 9), which can be visualized by X-ray topography.

This is also the case with another extended defect termed a *stacking fault*, which occurs when the stacking sequence of the lattice planes changes and part of the crystal has an orientation different from the rest (figure 10). A stacking fault is often the reason for twinning.

When large blocks of the crystal lattice are tilted slightly with respect to one another, an extended defect termed a *small-angle boundary* (figure 11) results. Similar defects are *growth sector boundaries*, which occur when portions of a crystal lattice growing along different respective lattice planes meet one another so as to generate a rough internal face, which often can be recognized on the crystal's surface as a seam. X-ray topography can depict such internal lattice boundaries.

The assemblage of internal extended lattice defects present is unique to any crystal. Hence, the lattice defect features of a particular diamond, rough or cut, render it unique. Most internal extended lattice defects are not visible in a gemological microscope, but they can be depicted by directing X-rays at the diamond's crystal lattice and recording the resulting diffraction pattern on X-ray sensitive film or with an electronic imaging device.

X-RAY DIFFRACTION

When X-rays are directed toward a crystal, they are diffracted; that is, part of the incident or "primary" X-ray beam is deflected into various directions by

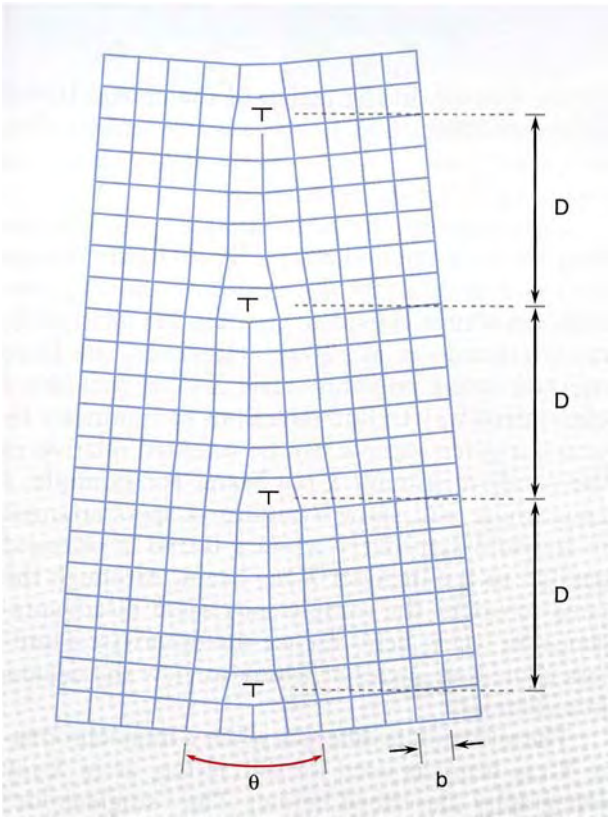

Figure 11. This diagram of a small-angle boundary shows an array of dislocations spaced by an average distance D (which is on the order of 10 nm to 1 µm). The angle θ between the two crystal regions typically measures between 0.01° and 1°. For each dislocation, the lattice planes are displaced by the distance "b."

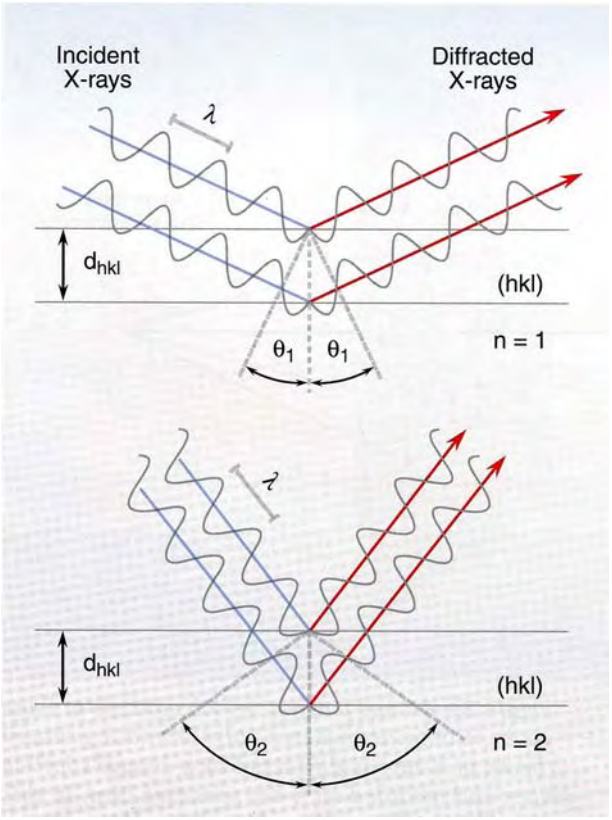

Figure 12. A monochromatic X-ray beam of wavelength λ is diffracted by a set of lattice planes (hkl) according to their spacing d_{hkl}. Different orders of X-ray diffraction can occur at various Bragg angles θ_1, θ_2, etc., according to the integer n, which is defined by the difference between the propagation lengths of the X-ray waves. Examples for n = 1 and n = 2 are shown here.

virtue of the crystal lattice (Cullity, 1978). This is because both the crystal-lattice spacings and the wavelength of X-rays are on the order of 0.1 nm. If the primary X-ray beam is composed of many wavelengths (a polychromatic or "white" X-ray beam), the diffracted beams expose an X-ray sensitive film with a pattern that represents the symmetry of the crystal lattice in the direction of the primary beam, a procedure called the *Laue method*.

Each diffracted beam is generated by the reflection of a small portion of the primary beam's range of wavelengths from a set of parallel lattice planes within a crystal. However, this reflection does not occur for any angle of incidence, but only at certain "glancing angles" (i.e., the angle between the incident X-ray beam and the set of diffracting lattice planes). This condition—"Bragg reflection" or "diffraction condition"—is given by the Bragg equation:

$$n\lambda = 2d_{hkl}\sin\theta_{hkl}$$

where: n = order of diffraction
λ = X-ray wavelength
d_{hkl} = distance between lattice planes
θ_{hkl} = Bragg angle

A polychromatic X-ray beam will produce many diffracted beams, each with a different wavelength and glancing angle. Therefore, many glancing angles are possible that satisfy the diffraction condition, thus generating a diffraction pattern. At a fixed glancing angle θ, an X-ray beam with a specific wavelength λ is diffracted according to the lattice plane spacing d_{hkl} (figure 12). The diffracting set of lattice planes has Miller indices (hkl), so the corresponding X-ray reflection is indexed hkl—without parentheses—and termed a *Laue index*. The resulting spot on the film is called a *Laue spot* (figure 13). The intensity of the diffracted X-ray beam is influenced by the lattice

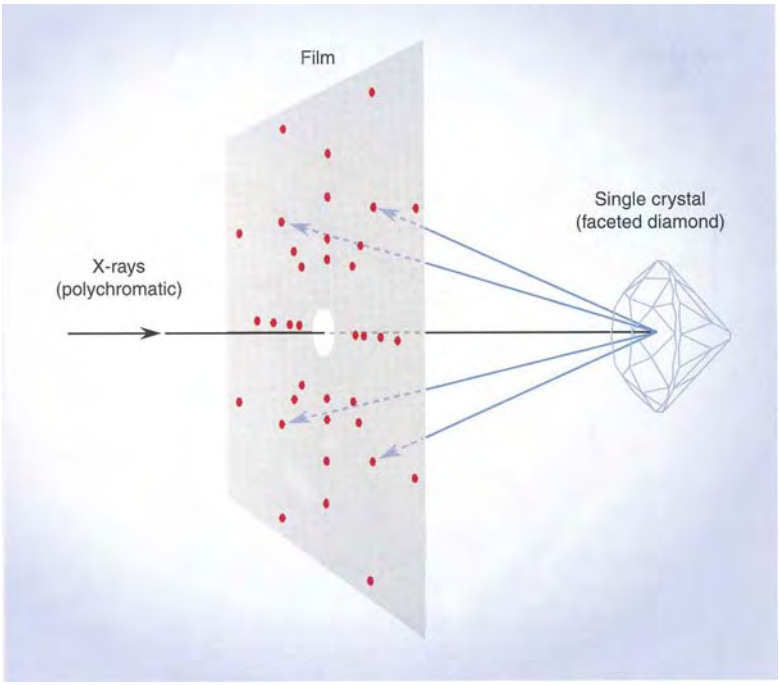

Figure 13. A Laue pattern, which consists of Laue spots, is obtained when a polychromatic primary beam of X-rays is diffracted by a crystal's lattice planes and recorded on X-ray sensitive film. In this "back-reflection" set-up, the film is oriented perpendicular to the primary beam, between the X-ray source and the sample. The primary beam is directed through a central hole in the film.

Figure 14. This diagram shows the diffraction geometry used for X-ray topography that was devised by Lang (1959). The crystal and recording medium are moved at the same time during the procedure, to record the spatial resolution of the lattice defect structure on the topograph.

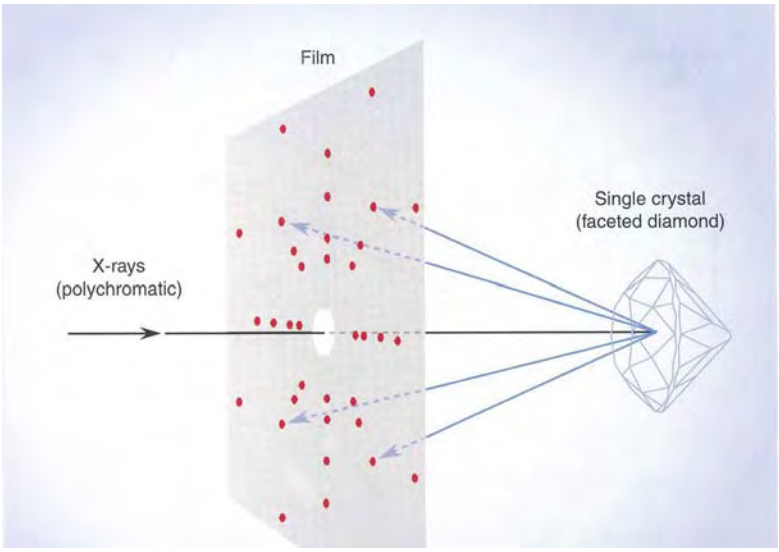

defects present in the region of the crystal lattice causing the diffraction. Hence, a spot recorded on the film contains information on the lattice defects in the form of intensity modulations.

Unfortunately, due to its limited spatial resolution, the Laue method cannot record lattice defects in sufficient detail for fingerprinting (unless a synchrotron source is used to generate the incident X-rays; Rinaudo et al., 2001). However, the Laue method (using polychromatic X-rays) provides a convenient way to find directions of symmetry by which a given sample can be oriented relative to the incident primary X-ray beam. For example, a Laue image will show a pattern of spots arranged in fourfold symmetry when a tetrad is oriented parallel to the incident X-ray beam. Although the need to orient the sample may seem disadvantageous, in fact it helps reduce the otherwise countless choices of angles at which to view the defects in a diamond.

The situation is different when a monochromatic X-ray beam is used for diffraction, as in X-ray topography (described below). The "single-color" radiation composing this beam has a specific wavelength λ (e.g., X-rays from a copper source have λ=0.154 nm), so the number of glancing angles under which "reflection" (diffraction) of the primary X-ray beam can occur is greatly reduced. The orientation of the crystal lattice relative to the incident X-ray beam must be carefully positioned to induce diffraction of the X-ray beam (i.e., to satisfy the Bragg equation).

X-ray diffraction occurs when the glancing angle (θ_1) is such that the difference between the propagation lengths of a set of parallel X-ray waves within the incident beam is an integer number "n" of wavelengths also called the *order of diffraction*. The case for n = 1 is shown in the upper part of figure 12, where the difference in the propagation lengths between both waves is just one wavelength λ. Diffraction also is observed at another glancing angle (θ_2), if n is a multiple of 1, such as 2—as shown in the lower part of figure 12, where the difference is 2λ. The corresponding Laue index is termed 2h 2k 2l to indicate the second order of diffraction. Thus, although Miller indices always consist of base integers, such as (110), higher-order reflections from the same set of lattice planes carry Laue indices such as 220, 330, etc., from which can be derived the Bragg angle under which diffraction is observed.

The X-rays most commonly employed in industrial laboratory diffraction experiments are generated

Figure 15. In the X-ray topographic apparatus used in this study, the diamond is held in the circular goniometer array (20 cm in diameter) in the top-center of the photo. The X-ray beam enters from the left, and the film is positioned on the right side of the goniometer. Photo by Nikolaus Herres.

using copper (λ=0.154 nm), molybdenum (λ=0.071 nm), or silver targets (λ=0.056 nm) in the X-ray tube. The shorter the wavelength λ is, the more energetic the X-rays are, and the deeper they can penetrate a sample.

X-RAY TOPOGRAPHY

The method of applying X-rays to image crystal lattice defects with local resolution is called *X-ray topography*, and the image recorded on a photographic plate is an *X-ray topograph*. X-ray topography of extended lattice defects in diamond was pioneered by A. R. Lang and co-workers (see, e.g., Frank and Lang, 1965; Lang, 1978b, 1979; Lang et al., 1992). Since diamond is highly transparent to X-rays, X-ray topography is particularly suited to imaging its lattice defects. Topographs can be taken irrespective of the stone's shape, and X-rays do not induce color change in a diamond. Hence, the method is nondestructive.

To obtain the greatest amount of information, the specimen is exposed to monochromatic X-rays according to a method devised by Lang (1959; figures 14 and 15). Slits are used to form the monochromatic X-ray beam into a ribbon-like shape some 10 μm thick and equal in height to that of the sample. The diamond is oriented relative to the incident X-ray beam such that a desired set of lattice planes satisfies the Bragg condition. An oscillating mount is used to expose all portions of the sample to the incident X-ray beam.

The image generated by the diffracted beam is recorded on the photographic plate (or on a screen when employing an electronic imaging device with a charged-coupled detector [CCD]). This image shows the locally resolved intensity of the diffracted X-ray beam as modified by the defects in the portion of the crystal lattice that is analyzed. In theory and, so far, in practice, no two diamonds have identical sets of defects (just as no two people have identical fingerprints). An X-ray topograph, therefore, provides a fingerprint that is unique to each particular diamond.

This is demonstrated by the X-ray topographs of a diamond crystal and the round brilliant cut from it (figure 16), and of a rough diamond that was cut first to a round brilliant, then recut to a smaller round brilliant, and ultimately recut again to a totally different shape (figure 17). The unique appearance of the extended lattice defects is clearly preserved through the faceting and recutting processes. Similarly, such defects should remain identifiable in topographs of diamonds taken before and after HPHT processing (as shown by Smith et al., 2000).

Diamonds with a low clarity grade will also show a large number of extended lattice defects, since fissures and inclusions locally destroy the

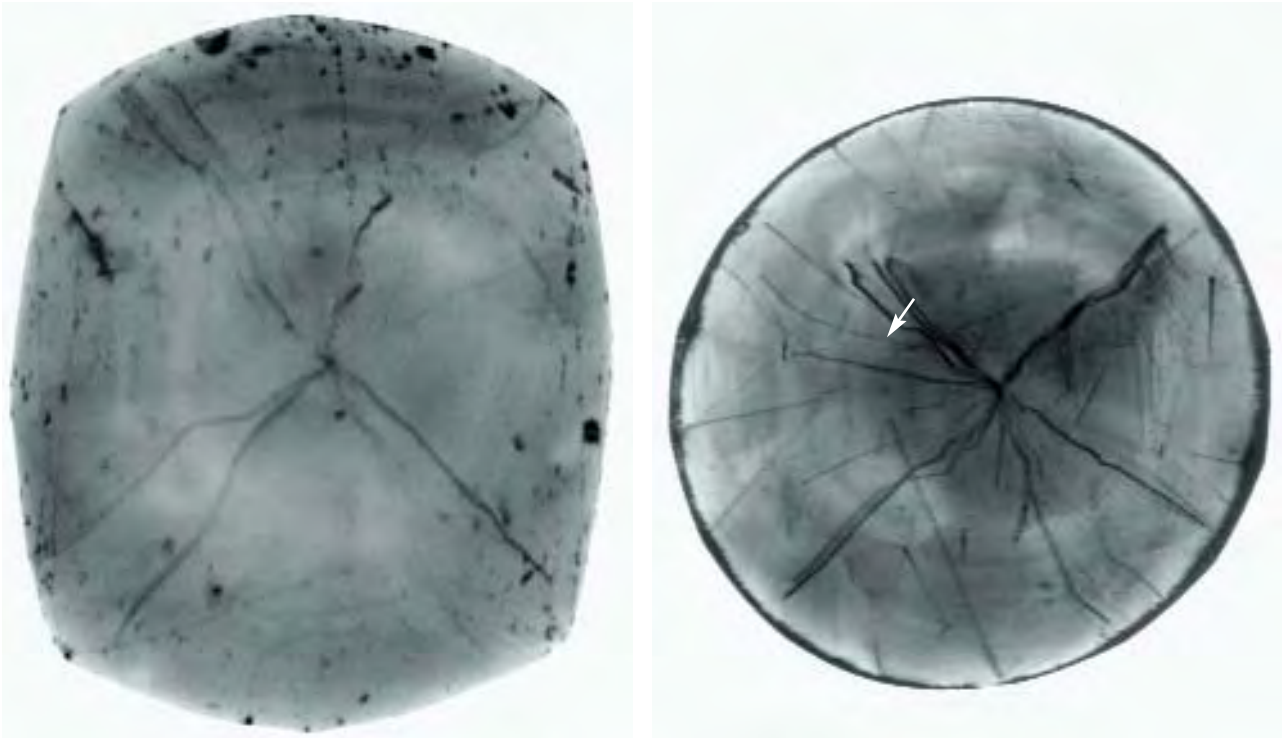

Figure 16. These X-ray topographs were taken of a 1.67 ct rounded diamond octahedron and a 0.75 ct round brilliant that was cut from it. Dislocations are seen as strong irregular lines originating from the center of the diamonds. In the rough sample, shades of gray indicate areas of different lattice strain and minute misorientations (i.e., deviation from the diffraction condition); surface blemishes appear as dark spots. In the faceted sample, the generally darker area that is slightly off-center marks an area of higher X-ray absorption through the stone's pavilion, which is the thickest part of the sample. Rough facet edges are visible as straight dark lines, and the location of the culet is shown with an arrow. The appearance of the dislocations in the two topographs differs somewhat because they would have been projected onto the film from different directions.

integrity of the crystal lattice. If the lattice defects are too abundant, their interference will render a topographic image rather meaningless. Although the image could still provide a fingerprint, it is unlikely that a stone of such low commercial value would be submitted for this procedure.

X-ray topography can also be used to identify natural vs. synthetic diamonds (see, e.g., Lang et al., 1992; Sunagawa, 1995; Martineau et al., 2004). This could become significant in the future, as diamond synthesis techniques are refined to produce larger, high-quality stones with less evidence of a synthetic origin (e.g., inclusions and luminescence features).

TYPICAL METHOD FOR GENERATING A TOPOGRAPH

To record X-ray topographs, one needs a set-up similar to the one diagrammed in figure 14. The diamond is mounted on an adjustable specimen holder that allows for translation and rotation of the sample in front of the X-ray beam. Taking X-ray topographs also requires proper choice of the Bragg reflection to be used for imaging. This selection is made by practical considerations. First, the cross-section of the stone that is projected onto the film should be as large as possible to minimize superposition of defects; in the case of a round brilliant, the projected image should thus be a circle. Second, the "diffracting power" of the selected set of lattice planes (i.e., the intensity of the diffracted X-ray beam) should be high, to reduce exposure time. In the case of diamond, Bragg reflections of the 220 type satisfy both conditions (Lang and Woods, 1976).

The diamond is oriented according to the desired glancing angle θ_{220} by using X-ray diffraction to locate an appropriate crystallographic reference vector—such as a tetrad or diad. This reference vector can be found through the use of the sample holder, actually a *goniometer*, which has a number of circles that rotate on independent axes. Figure 18 shows a goniometer with five circles, denoted A through E. The desired reference vector is found by

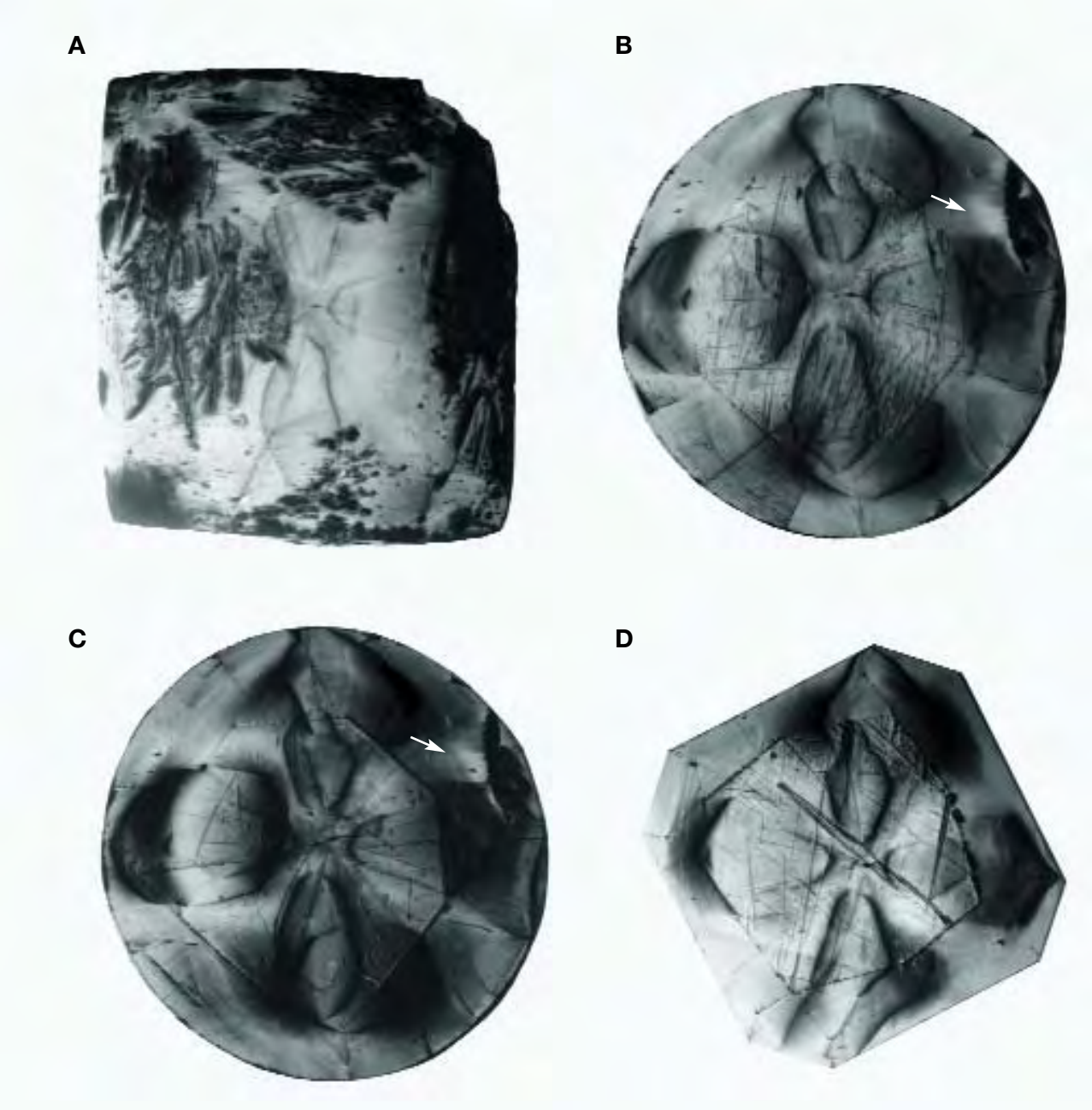

Figure 17. This sequence of topographs was taken from the same diamond in rough, cut, and recut states. Topograph A was taken from a 2.31 ct half-octahedron, which was faceted into the 1.19 ct round brilliant shown in topograph B. A defect structure determined by growth sector boundaries shaped like a four-leaf clover is clearly visible, as is a small inclusion near the upper right edge (marked by an arrow). This stone was then slightly recut to 1.12 ct, which has a nearly identical topograph (C); note the difference in the surface features. The diamond was then completely recut to a 0.88 ct square shape (Sunflower Carré; topograph D), with the inclusion removed in the process. (The diagonal linear feature near the center of topograph D corresponds to a scratch on the table facet.) Even after extensive recutting, the typical internal features in this diamond remain recognizable, linking it to the round brilliants as well as the original rough. The light and dark areas in topograph D are distributed somewhat differently due to the modified absorption behavior of X-rays in the Sunflower cut.

applying a search procedure with systematic rotational movements around the goniometer circles. A set of suitable symmetrically equivalent reflections such as 220, $2\bar{2}0$, $\bar{2}\bar{2}0$, and $\bar{2}20$ eventually is located and then is precisely aligned using the X-ray detector mounted on circle E.

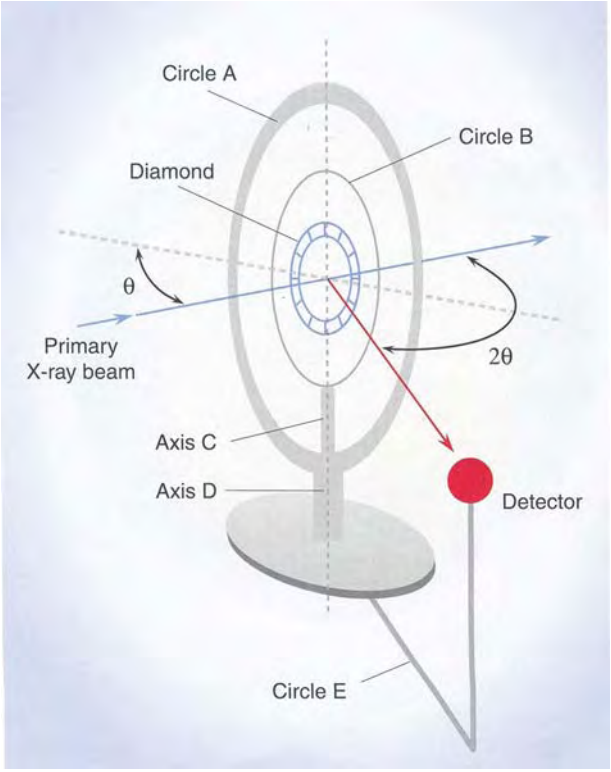

Figure 18. A five-circle goniometer was used to crystallographically align the diamonds prior to recording X-ray topographs. The five circles are preferably driven by computer-controlled motors. The diamond is attached in the center of the goniometer with its table facet perpendicular to the primary X-ray beam. The detector is used for adjusting, aligning, and measuring the reflecting position and the polar angles ρ and φ. To record a topograph, the detector is replaced by a camera or other imaging device.

This search procedure can be executed manually or, more readily, via fully automatic computer control with special software. In the end, the diamond is positioned so that a crystallographic reference vector such as a tetrad is oriented parallel to the goniometer's A-axis (around which the A circle rotates). The detector is then removed and replaced with a photographic plate or imaging assembly to record a topographic image.

Knowing the glancing angles of the 220-type Bragg reflections and now their positions, images using the four symmetrically equivalent Bragg reflections can be taken one at a time. Although they are taken of the same set of lattice defects, the topographs differ slightly because the defects have been projected onto the film from four different directions. Figure 16 shows a topograph where the pavilion facet edges are clearly seen, with the culet off-center.

PAST LIMITATIONS OF THE TECHNIQUE

The unique and hence unambiguous characterization of rough, partially cut, or fully cut gem diamonds by means of X-ray topography has been known for some years (Lang and Woods, 1976; Diehl, 1982; Sunagawa et al., 1998). Fingerprinting diamonds via X-ray topographic images of their lattice defects has been used to relate cut diamonds to their parent rough (Lang, 1975, 1978a, 1988; Lang and Woods, 1976; Sunagawa et al., 1998). So far, however, the method has not been applied systematically as a "passport" for individual fashioned diamonds, and the diamond trade has not yet seen widespread use of this fingerprinting technique, even for gem diamonds of high value. What are the reasons?

One reason is simply the difficulty of obtaining a well-defined topograph from a faceted diamond. Directing the monochromatic X-ray beam perpendicular to the table facet will not necessarily yield a Bragg reflection, since it is unlikely that this arbitrarily chosen orientation yields an angle θ that satisfies the diffraction condition. Even if a glancing angle is found, the beam will not necessarily diffract in the direction of the photographic plate. Therefore, one first has to solve the problem of precisely orienting the stone relative to the incident X-ray beam, which is done using X-ray diffraction and a goniometer.

Moreover, due to the high crystallographic symmetry of the diamond lattice, there are many symmetrically equivalent Bragg reflections available to record an X-ray topograph. For example, there are 12 symmetrically equivalent type 220 reflections that share the same value for d_{220} and hence the Bragg angle θ_{220}. Thus, a complete characterization of a diamond requires the recording of at least 12 X-ray topographs (referred to as "mother topographs") in order to provide indisputable proof of identity when compared to a single ("daughter") topograph taken later for re-identification.

It is important to remember that a single lattice defect within a given diamond can have a variable appearance when viewed from different directions, just as a car looks different when viewed from above, below, and the side. Although each of the symmetrically equivalent Bragg reflections has the same diffraction condition, each also has a different projection orientation, which will cause the corresponding topographs to look different.

Even using the same Bragg reflection, the topograph projected along one direction may significantly differ from the topograph obtained in the reverse

direction, because of differences in the volume of the diamond that is penetrated by the X-rays. Imagine an extended lattice defect that penetrates the surface of the stone. The diffracted beam that carries the image through the volume of the stone will suffer from some absorption and scattering, so the projected image may appear somewhat blurred on the photographic plate, and the low-contrast surface features may even become invisible. In the reverse direction, the defect image is generated just before the diffracted beam leaves the stone, so the image (and even the low-contrast surface features) will appear sharper on the photographic plate. So, using the Bragg reflection of type 220, 24 topographs may actually be needed to characterize a single diamond.

The execution of this procedure would require highly trained personnel and considerable effort in labor and time, so that the corresponding costs would be prohibitive. This is why X-ray fingerprinting of gemstones, although highly desirable for property protection, has not yet become commercially viable. So far, X-ray fingerprinting of diamonds, as well as other gem materials (Rinaudo et al., 2001), has remained a matter of research.

Figure 19. The diagram on top shows an example of how the table facet cuts through a diamond's crystal lattice. A line perpendicular to the table facet (T) forms angles with the three tetrads (axes of four-fold symmetry). Shown here is the tetrad that forms the smallest angle with T. The drawings below illustrate how octahedral diamond crystals are commonly sawn during preforming, in a direction that is approximately parallel to a cube direction.

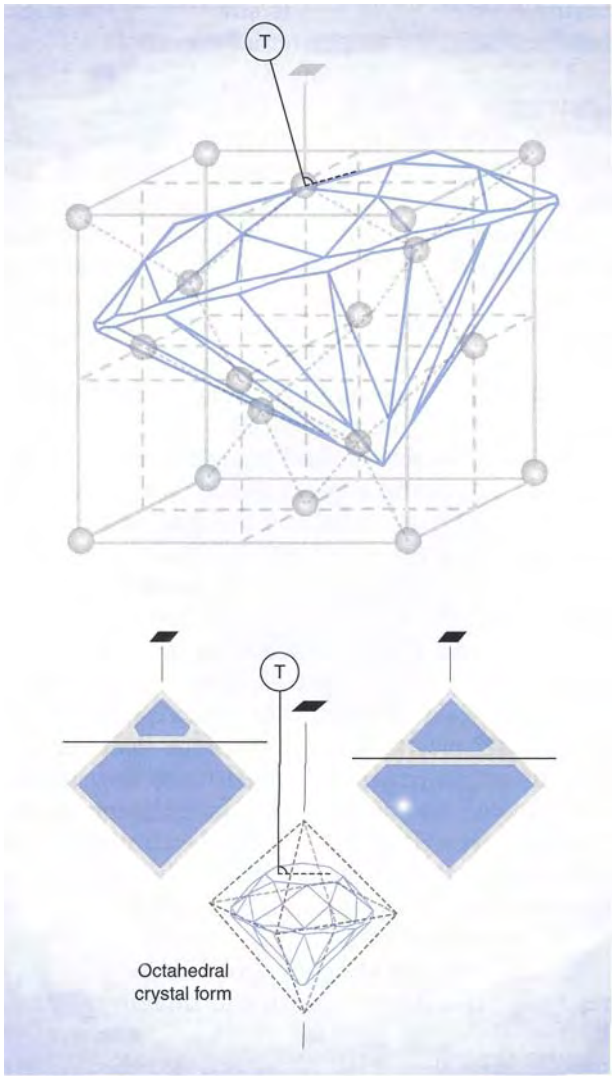

EXECUTION OF THE SIMPLIFIED ROUTINE

One way to make X-ray topography commercially viable would be to drastically reduce the number of mother topographs required to identify a faceted diamond. If the sample could be uniquely and reproducibly aligned in front of the X-ray source (e.g., relative to the table facet), only one mother topograph would be needed. This section describes such a procedure, as developed and patented by us (see Diehl and Herres, 1997; 1998). We used the table (as the most prominent facet of a cut diamond) to begin the alignment. Using X-ray diffraction, we started with the table perpendicular to the primary X-ray beam, and searched for the tetrad forming the smallest angle with the perpendicular T to the table facet (figure 19). This is the first part of the routine to determine the orientation of the table facet relative to the diamond lattice.

Many rough diamonds are octahedra or dodecahedra, which are sawn along a cube direction to yield a larger and a smaller rough diamond (again, see figure 19). The cross-sectional surfaces—which later become the table facets of the two gems—are thus nearly perpendicular to a tetrad of the diamond lattice. As a result, for many faceted diamonds, a tetrad is approximately perpendicular to the table facet (usually within 10°).

When this closest tetrad is selected as the crystallographic reference vector for recording topographs, the plane of the faceted diamond's girdle is projected onto the X-ray topograph with minimum distortion so that the projected area and thus the information content of the topograph are maximized. If a tetrad is

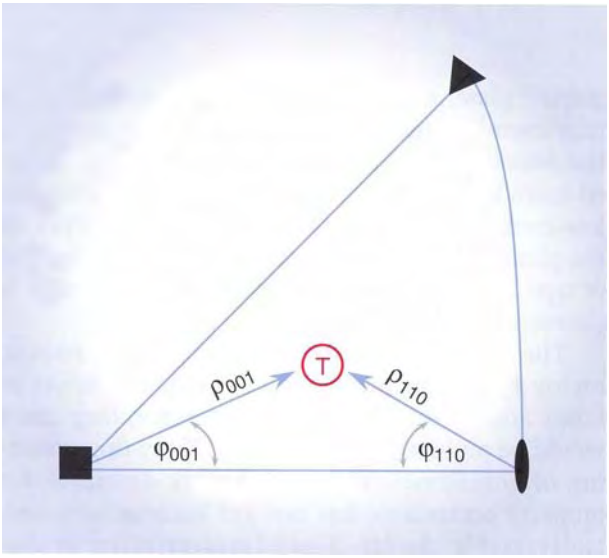

Figure 20. The position of the pole belonging to the perpendicular to the table facet (T) can be represented by the stereographic projection of this pole within the standard triangle t. If the chosen reference direction is a tetrad, the azimuth and polar distances are φ_{001} and ρ_{001}, respectively. If the reference direction is a diad, they are φ_{110} and ρ_{110}.

not found within a preset angular range, our automated procedure will then look for a diad. Since, in most cases, the crystal vector closest to the perpendicular T to the table facet will be a tetrad, we will describe the alignment procedure for this orientation. Figures 8 and 18 may help clarify the following description of the procedure we have developed.

To search for the diffraction condition for the set of 001 lattice planes to which the tetrad is perpendicular, the specimen is placed in the center of the goniometer and systematically moved using circles B and C. The detector finds and optimizes the signal for the strong 004 reflecting position, so that a tetrad is aligned perpendicular to circle A. This tetrad indicates the direction of one of the cubic coordinate axes, which we arbitrarily assign as a_3 (i.e., the vector [001] in the diamond lattice).

The second part of the alignment routine uses the 220 Bragg reflection to establish a unique orientation of the stone for taking the X-ray topograph—that is, we find and set the azimuthal orientation (see below) necessary to start the imaging. Circles D and E are set to include the Bragg angle of the diamond 220 reflection. Circles B and C remain fixed at the positions found before. The sample is rotated using circle A in order to find and optimize the signal for the 220-type reflecting positions.

The stereographic projection on the left in figure 8 illustrates that we should be able to find four 220-type reflecting positions (corresponding to the four diads at the rim). We now single out one of these four symmetrically equivalent reflections by optimizing only the 220-type reflection position of the set of 110 lattice planes, which has the perpendicular vector [110] that forms the smallest angle with T. We arbitrarily refer to this Bragg reflection as "220," and this is the one used to record the mother topograph.

For diamonds cut from irregularly shaped rough, the table may be oriented quite differently from that of a gem derived from an octahedron or dodecahedron. This may lead to larger angles between T and the closest tetrad. In order to retain a large projected area of the stone (e.g., a circle in the case of a brilliant), it may be more practical to use a diad, instead of a tetrad, for the reference vector that is nearest to T. Since a tetrad has an angle of 45° with its neighboring diads, using a diad is advisable if the angle between T and the closest tetrad exceeds 22.5°.

In either case, after the X-ray diffraction alignment procedure is complete, the geometric relationship between T and the closest tetrad (or diad) is measured in terms of two crystallographic angles, namely the azimuth φ and the polar distance ρ (figure 20).

Imagine, with the help of figure 7, that this tetrad or diad coincides with the vertical line through the center of the sphere. T will then form a pole somewhere on the surface of the sphere. By definition, the stereographic projection of this pole will be found in the standard triangle t displayed in figure 8 and enlarged in figure 20.

As shown in the standard triangle of figure 20, the azimuth φ_{001} is the angle between two planes: the first defined by the tetrad and the diad, and the second containing the tetrad and T. The polar distance ρ_{001} is the angle between the tetrad and T. When using a diad, the assignment of φ_{110} and ρ_{110} is done in a similar way. Common ranges for φ and ρ are 0–45° and 0–22.5°, respectively. Using the goniometer and the X-ray detector, both angles can be recorded with high precision (usually to better than $^1/_{10}$°).

This alignment routine determines how to orient a faceted diamond prior to taking the topograph. The two crystallographic angles—azimuth φ and polar distance ρ—uniquely define the position of the table facet with respect to the underlying diamond crystal lattice.

Finally, the mother topograph is recorded by replacing the detector with the imaging device. Because the orientation is unique, only one mother topograph is required. In the event that the identity

of a diamond needs to be verified, the same routine is executed by reproducing both crystallographic angles to record the new topograph. If it is the same stone, the alignment angles should be equal within the goniometer's tolerances (±0.2°), and the daughter topograph will show unique features that are recognizable in the mother topograph (again, see figures 16 and 17).

DISCUSSION

We have endeavored to present here a viable technique, together with its underlying principles, to render X-ray fingerprinting a practical tool for the identification of individual cut diamonds. The technique involves imaging the lattice defect structure of a faceted diamond under specific, well-defined, reproducible conditions. This is made possible by measuring the polar angles φ and ρ.

Figure 21. As illustrated here, a fingerprint generated by this X-ray topography routine could accompany a diamond grading certificate. The polar angles and X-ray topograph provide complementary information that is unique to a particular faceted diamond. (MoKα denotes the X-ray wavelength of highest intensity from a molybdenum target.)

Polar Angles φ and ρ. The azimuth φ and polar distance ρ are typically unique to every faceted diamond. Together, these two angles define the orientation of a specimen's table facet with respect to its crystal lattice in terms of a reference direction (nearest tetrad or diad). Within the alignment tolerances of the goniometer, both polar angles are reproducible and almost always unique. Therefore, although they are obtained as a "by-product" during the alignment procedure for taking topographs, the polar angles contribute further valuable information for fingerprinting a stone. Particularly in combination, the polar angles are highly characteristic in their own right. Being numerical values, they also may serve as searching parameters to quickly locate the potential mother topograph in a database. Using suitable software, the search can be performed automatically.

It is important to note that the polar angles would become useless for fingerprinting if the inclination angle of the table facet relative to the diamond crystal lattice is modified significantly. However, this would occur only if there were some significant reshaping of the stone, as well as appreciable loss of weight.

X-ray Topographs. The mother X-ray topograph provides a unique, archivable diamond fingerprint. Such fingerprints reproduced on microfilm could become an integral part of a diamond report (e.g., as in figure 21), with a digital copy archived separately. Should a stone be recovered after loss or theft, its "fingerprint" could be compared to that of the mother topograph to confirm identity.

Properly oriented, daughter and mother topographs from the same diamond will be identical with respect to the image characteristics stemming from internal defects. Even two diamonds cut from the same rough can clearly be differentiated, according to subtleties in their defect structure, as well as their polar angles. Complete reproduction of all details, such as polishing flaws and rough or damaged facet edges, would be achieved only if the diamond had not been repolished after the mother topograph was recorded. Significant recutting would be expected to remove some features of the fingerprint, while leaving the rest intact. If the table facet's inclination angle is changed by only a few degrees, a daughter topograph will differ only slightly from the mother topograph. Extensive reshaping would complicate the identification, although it is still possible in principle (see, e.g., figure 17). In the worst-case

scenario, multiple (up to 24) X-ray daughter topographs would be needed to prove that a diamond was recut from a particular stone. This also would require experience in interpreting the features visible on the topographs. Nevertheless, such effort would be worthwhile in exceptional cases.

The exposure time is an important consideration, since it affects topographic contrast. If the recording conditions are identical, mother and daughter topographs will be identical. The exposure time depends on the flux of X-rays. Efforts should be made to standardize the X-ray flux according to sample size, orientation, and the like.

In rare cases, a diamond's topographic fingerprint may not be diagnostic. For example, samples with a very low concentration of extended defects might yield only a few useful features. In contrast, diamonds with very high concentrations of defects could render X-ray topographs meaningless due to multiple superpositions of defects. In both cases, however, the polar angles might prove useful as identifiers. In unusual cases in which the reference direction is exactly perpendicular to the table facet, more than one mother topograph must be recorded. In such a case, a maximum of four topographs are needed if the reference direction is a tetrad, or a maximum of two for a diad. Nevertheless, only one daughter topograph will be needed for comparison.

What is the size range of diamonds that can be fingerprinted by X-ray methods? So far, we have been unable to obtain large diamonds for testing this technique; the largest sample weighed 2.31 ct and was 5.1 mm in thickness (figure 17). The penetration depth of X-rays into diamond depends on the energy of the incident X-rays. From data on absorption and extinction of X-rays when interacting with matter (see, e.g., Wilson, 1992), we have derived some reasonable estimates for acceptable stone sizes. Employing X-rays from a copper target, diamonds with a thickness of up to 3 mm can be topographed. For molybdenum and silver radiation, the maximum thicknesses are estimated at 8 mm and 12 mm, respectively. For thicker samples, the defect contrast would become weaker due to increasing absorption, and even larger sizes would not be expected to show distinctive topographs due to the superposition of too many defects (unless the defect concentration is low). Nevertheless, some fingerprinting of larger diamonds can be accomplished by using their polar angles and also by observing topographic features near the edges where the thickness is reduced.

APPLICABILITY TO THE GEM TRADE

To establish an X-ray topographic fingerprinting laboratory, a floor space of about 10 m^2 and the necessary means to run an X-ray generator (e.g., water cooling) are required. A minimum investment of approximately US$50,000 is envisaged, to purchase an X-ray generator with a stationary anode, a multiaxes goniometer with stepping motors, computer, printer, and the like. A darkroom for film processing is not needed, as digital X-ray imagers with high sensitivity and acceptable resolution have become available (see, e.g., www.photonic-science.ltd.uk). This allows for short exposure times and the observation of topographs while the sample is still positioned in the goniometer. Costs for X-ray imaging systems are in the range of $15,000–$35,000, depending mainly on the size and resolution of the imaging chip.

Software development costs for computer automation of the equipment and programming are estimated at $25,000. After a straightforward routine has been implemented, it should take 6–20 minutes to acquire each topograph. Operating expenses, outside of the space required, are relatively small, involving primarily water use (coolant), electricity, and salaries. Technical personnel need not have a scientific background because specific knowledge and expertise are incorporated into the software.

The routine described here can be executed in any laboratory competent in X-ray crystallography. Such laboratories are found in many research institutes that are active in materials science, solid-state physics, crystal chemistry, and earth sciences. Since the investment costs are relatively high and a secure infrastructure is required, only major gem laboratories would be expected to consider this X-ray fingerprinting procedure. Ideally, these laboratories would develop a workable agreement to share their databases over the Internet. The pole angles could serve as searching parameters to quickly locate mother topographs in a database.

The simplified routine for the X-ray diffractive/topographic characterization of faceted diamonds presented here considerably reduces the time, effort, and manpower needed for fingerprinting diamonds. The polar angle data and the mother topograph could make valuable additions to a diamond's certificate, providing added confidence for both the jeweler and the consumer.

ABOUT THE AUTHORS

Dr. Diehl (rodiehl@t-online.de) is senior scientist at the Fraunhofer Institute for Applied Solid-State Physics IAF in Freiburg, Germany, and is an advisory board member of the German Gemmological Association in Idar-Oberstein. Dr. Herres (nikolaus.herres@ntb.ch) is a lecturer at the Interstaatliche Hochschule für Technik NTB in Buchs, Switzerland.

ACKNOWLEDGMENTS: The authors express their sincerest thanks to Karl-Heinz Meng of Idar-Oberstein for providing diamond specimens for examination and development of the method described in this article. They are also deeply indebted to Lutz Kirste (Fraunhofer IAF) for his support in providing access to the equipment and for taking several of the X-ray topographs.

REFERENCES

Bohm J. (1995) *Realstruktur von Kristallen*. Schweizerbart'sche Verlagsbuchhandlung, Stuttgart, Germany.

Borchardt-Ott W. (1997) *Kristallographie*, 5th ed. Springer-Verlag, Berlin, Germany.

Buerger M.J. (1967) *Elementary Crystallography*. Wiley, New York.

Cullity B.D. (1978) *Elements of X-Ray Diffraction*, 2nd ed. Addison-Wesley, Reading, Massachusetts.

Diehl R. (1982) Möglichkeiten der Edelsteindiagnose mit Hilfe der Röntgentopographie [Possibilities of gem identification using X-ray topography]. *Zeitschrift der Deutschen Gemmologischen Gesellschaft*, Vol. 31, pp. 3–22.

Diehl R., Herres N. (1997) *Verfahren zur röntgenographischen Identifizierung von geschliffenen Diamanten* [*X-Ray Identification Method for Cut Diamonds*]. German patent DE 1963 1367, issued November 13.

Diehl R., Herres N. (1998) Ein vereinfachtes Verfahren zur zweifelsfreien Identifizierung von geschliffenen Diamanten. *Gemmologie: Zeitschrift der Deutschen Gemmologischen Gesellschaft*, Vol. 47, No. 2, pp. 77–88.

Frank F.C., Lang A.R. (1965) X-ray topography of diamond. In R. Berman, Ed., *Physical Properties of Diamond*, Clarendon Press, Oxford, England, pp. 69–115.

Kelly A., Groves G.W., Kidd P. (2000) *Crystallography and Crystal Defects*, revised ed. Wiley, Chichester, England.

Lang A.R. (1959) A projection topograph: A new method in X-ray diffraction microradiography. *Acta Crystallographica*, Vol. 12, pp. 249–250.

Lang A.R. (1975) *Diamond Identification*. British patent 328/75, issued January 3.

Lang A.R. (1978a) *Diamond Identificatio*n. U.S. patent 4,125,770, issued November 14.

Lang A.R. (1978b) Techniques and interpretation in X-ray topography. In S. Amelinckx et al., Eds., *Diffraction and Imaging Techniques in Material Science*, Vol. II, North-Holland, Amsterdam, pp. 623–714.

Lang A.R. (1988) *Verfahren zur Identifizierung von Diamanten*. German patent DE 2559245 C2, issued May 26.

Lang A.R. (1979) Internal Structure. In J.E. Field, Ed., *The Properties of Diamond*, Academic Press, London, pp. 425–469.

Lang A.R., Woods G.S. (1976) Fingerprinting diamonds by X-ray topography. *Industrial Diamond Review*, March, pp. 96–103.

Lang A.R., Moore M., Walmsley J.C. (1992) Diffraction and imaging studies of diamond. In J.E. Field, Ed., *Properties of Natural and Synthetic Diamond*, Academic Press, London, pp. 215–258.

Laurs B.M., Ed. (2001) Gem News International: White House conference on "conflict" diamonds. *Gems & Gemology*, Vol. 37, No. 1, pp. 64–66.

Martineau P.M., Lawson S.C., Taylor A.J., Quinn S.J., Evans D.J.F., Crowder M.J. (2004) Identification of synthetic diamond grown using chemical vapor deposition (CVD). *Gems & Gemology*, Vol. 40, No. 1, pp. 2–25.

McKie D., McKie C. (1974) *Crystalline Solids*. Nelson, London.

Moses T.M., Shigley J.E., McClure S.F., Koivula J.I.., Van Daele M. (1999) Observations on GE-processed diamonds: A photographic record. *Gems & Gemology*, Vol. 35, No. 3, pp. 14–22.

Rinaudo C., Capelle B., Navone R. (2001) A new method to identify a cut gemstone. *Gemmologie: Zeitschrift der Deutschen Gemmologischen Gesellschaft*, Vol. 50, No. 1, pp. 43–50.

Smith J.G.C. (1999) *Diamond or Gemstone Marking by Plurality of Grooves*. European patent WO99/33671, issued July 8.

Smith C.P., Bosshart G., Ponahlo J., Hammer V.M.F., Klapper H., Schmetzer K. (2000) GE POL diamonds: Before and after. *Gems & Gemology*, Vol. 36, No. 3, pp. 192–215.

Sunagawa I. (1995) The distinction of natural from synthetic diamonds. *Journal of Gemmology*, Vol. 24, No. 7, pp. 485–499.

Sunagawa I., Yasuda T., Fukushima H. (1998) Fingerprinting of two diamonds cut from the same rough. *Gems & Gemology*, Vol. 34, No. 4, pp. 270–280.

Wallner, H.F., Vanier, D.J. (1992) *Gemstone Identification, Tracking and Recovery System*. U.S. patent 5,124,935, filed Nov. 30, 1990.

Wilson A.J.C., Ed. (1992) *International Tables for X-Ray Crystallography, Vol. C.* Publ. for the International Union of Crystallography by Kluwer Academic Publishers, Dordrecht, The Netherlands.